



ELSEVIER

Journal of Crystal Growth 175/176 (1997) 1009–1015

JOURNAL OF **CRYSTAL  
GROWTH**

## Continuously graded buffers for InGaAs/GaAs structures grown on GaAs

A. Bosacchi<sup>a</sup>, A.C. De Riccardis<sup>a</sup>, P. Frigeri<sup>a</sup>, S. Franchi<sup>a,\*</sup>, C. Ferrari<sup>a</sup>, S. Gennari<sup>a</sup>, L. Lazzarini<sup>a</sup>, L. Nasi<sup>a</sup>, G. Salviati<sup>a</sup>, A.V. Drigo<sup>b</sup>, F. Romanato<sup>b</sup>

<sup>a</sup> *CNR, MASPEC Institute, Via Chiavari 18a, I-43100 Parma, Italy*

<sup>b</sup> *INFN, Physics Department of Padova University, Via Marzolo 8, I-35131 Padova, Italy*

### Abstract

We report on the preparation under optimized conditions and on the study of InGaAs buffers grown on GaAs, intended for MQW structures for 1.3 and 1.5  $\mu\text{m}$  optical operation at 300 K; the buffers have linear, square-root and parabolic composition profiles. They were designed so that MQWs grown atop the buffers are virtually unstrained, unlike those prepared following the conventional approach that are under compressive strain. The results obtained by the concomitant use of TEM, HRXRD, AFM and PL show that, by carefully designing the buffers: (i) the misfit dislocation (MD) profiles and thicknesses of the MD-free regions in the buffers can be predetermined, (ii) active structures atop the buffers are virtually unstrained and have efficient 300 K photoluminescence in the 1.3 and 1.5  $\mu\text{m}$  windows of photonic interest, (iii) the structures have threading dislocation concentrations in the low  $10^6 \text{ cm}^{-2}$  range and show smooth and symmetric cross-hatchings.

### 1. Introduction

Lattice mismatched structures have interesting applications in spite of the potentially adverse effects related to strain relaxation, since they allow to extend the range of materials that can be considered and, then, of the properties that can be exploited. Moreover, the accurate control of the resulting strain may give significant advantages,

since it can be used as a tool for band engineering. Furthermore, it is of interest to use substrates that, even if mismatched: (i) have higher crystalline perfection and definite electrical, optical and mechanical properties, or (ii) allow the preparation of structures suited for the fabrication of different devices with integrated functions. Structures consisting of InGaAs layers deposited on GaAs substrates are gaining increasing attention for optical modulators based on the quantum-confined Stark effect [1], quantum well infrared detectors [2] and metamorphic high electron mobility transistors [3], 1.3  $\mu\text{m}$  quantum well lasers [4] and non-linear optical devices [5].

\* Corresponding author. Fax: + 39 521 269 209; e-mail: franchi@prmasp.bo.cnr.it.

Buffer layers with either step-graded or continuously graded compositions have been proposed to (i) relax the strain resulting from lattice mismatch; (ii) bury the misfit dislocations (MD) away from the active part of the structure; (iii) prevent the onset of three-dimensional nucleation; and (iv) reduce the propagation of threading dislocations (TD) towards the active parts of devices [6]. Linearly graded buffers are generally used (with the exception of Refs. [7, 8]), however, we expect that continuously graded buffers with selected composition profiles may give additional benefits, such as the control of the MD profiles within the buffers.

The aim of this work was to evaluate buffers with compositions graded according to (a) linear, (b) square-root and (c) parabolic (with the vertex at the top of the buffer) dependences on the distance from substrates. The experimental results were obtained by the concomitant use of transmission electron microscopy (TEM), high-resolution X-ray diffraction (HRXRD), atomic force microscopy (AFM) and photoluminescence (PL). The results show that by proper buffer designing: (i) the thicknesses of the MD-free regions of buffers can be varied, (ii) the MDs can be concentrated far from the active structures grown atop the buffers, (iii) these structures are virtually unstrained, (iv) the TD concentrations can be reduced in the low  $10^6 \text{ cm}^{-2}$  range, (v) the structures grown under optimized conditions have smooth and symmetric cross-hatchings and (vi) the MQWs have efficient 300 K photoluminescence in the 1.3 and 1.5  $\mu\text{m}$  spectral windows.

## 2. Experimental procedure

After careful studies on the optimization of growth conditions, the InGaAs buffers with different composition profiles were grown on semi-insulating (0 0 1) GaAs by solid-source MBE at 400°C using  $\text{As}_2$  beams; instead, the InGaAs/GaAs MQWs were grown at 400°C by atomic layer MBE (ALMBE) that allows to select the compositions of the InGaAs wells by only adjusting the In and Ga supply times, without changing the temperature of the cation cells reached at the end of the growth of buffers [9]. Composition grading was obtained by

varying the In and Ga cell temperatures in such a way to maintain a growth rate of 0.28 nm/s. Prior to each run, the In and the Ga fluxes were calibrated by RHEED oscillation measurements using InAs and GaAs substrates, respectively. The substrates were radiatively heated at growth temperatures  $T_g$  measured by a suitable optical pyrometer for  $T_g \geq 450^\circ\text{C}$  and by a thermocouple (TC) for  $T_g < 450^\circ\text{C}$ . For  $T_g < 450^\circ\text{C}$ , the TC readings were corrected by the difference ( $\sim 200^\circ\text{C}$ ) between the TC and the optical pyrometer values measured at  $T_g > 450^\circ\text{C}$ . Great care was paid to keep the growing surface temperature at the intended value during growth; this was done by lowering the electrical power to the substrate heater in a controlled way so as to counterbalance the increasing optical power absorbed during the growth of buffers and MQWs. The  $\text{As}_2$  beam-equivalent pressure (BEP) was  $5.5 \times 10^{-6}$  Torr, while the  $\text{As}_2/\text{Ga}$  BEP ratio was  $\sim 9$ .

TEM observations were carried out by an JEOL 2000FX instrument operating at 200 KeV on (1 1 0) oriented cross sectional samples. The dislocation distribution at the buffer/substrate interfaces and across the buffer layers was studied under bright field, dark field and weak beam conditions using  $g = 220$  type scattering vectors. Conventional  $g \cdot b$  contrast analyses showed that the majority of the dislocations were  $60^\circ$  type in character. Dark field  $g = 200$  type imaging conditions were used for studying the MQW structural quality and thicknesses. Finally, the MQW periods and interface-smoothness were studied in the lattice resolution mode.

High-resolution X-ray diffraction (HRXRD) measurements were performed using a diffractometer fitted with a four-crystal X-ray monochromator. (0 0 4) symmetrical and (3 3 5) asymmetrical  $\text{CuK}\alpha$  diffraction profiles were used to measure the strain and tilt angle of the MQWs; from these curves we also obtained the average lattice parameters of MQWs parallel and perpendicular to the interfaces, the compositions of the top of buffers and the average compositions and the period of MQWs. A good agreement between MQW periods determined by TEM and HRXRD was found, while the mean compositions of MQWs deduced by HRXRD are close to those determined

by Rutherford back-scattering experiments in selected samples.

Atomic force microscopy (AFM) was carried out under conventional conditions.

The photoluminescence (PL) spectra were taken at 10 and at 300 K with a spectral resolution of 0.5 meV, and were excited by the blue line of an Ar<sup>+</sup> laser, using power densities as small as 0.5 W/cm<sup>2</sup>.

### 3. Design of the structures

According to the existing models on strain relaxation [6, 8, 10, 11] buffers with increasing compositions can be divided into two parts: (i) the one closest to the substrate (up to a distance  $\delta_r$  from the substrate itself) is fully relaxed, due to the formation of misfit dislocations that have a concentration proportional to the composition gradient, and (ii) the topmost part that (a) is void of misfit dislocations, (b) has a lattice parameter  $a(x_r)$ , where  $x_r = x(\delta_r)$  ( $x(\delta)$  giving the dependence of the  $\text{In}_x\text{Ga}_{1-x}\text{As}$  composition on the distance  $\delta$  from the substrate and  $a(x)$  being the lattice parameter as a function of  $x$ ), and (c) is under strain in regions where  $x(\delta) \neq x_r$ . The values of  $\delta_r$  can be found by means of the equation [8, 10, 11]

$$k_n = \left(\frac{\Delta a}{a}\right)^n \int_{\delta_r}^{\delta_b} (x(\delta) - x(\delta_r))^n d\delta \quad (1)$$

with  $n = 1$  [10] or  $n = 2$  [8, 11];  $\Delta a/a = 0.07$  is the lattice mismatch between InAs and GaAs, while  $k_1 = 0.83 \text{ nm}$  [10],  $k_2 = 3.68 \times 10^{-3} \text{ nm}$  [8, 11] and  $\delta_b$  is the total thickness of the buffer.

From Eq. (1) it follows that by choosing the composition profile  $x(\delta)$  and the thickness  $\delta_b$  it should be possible to predetermine (i) the thickness ( $\delta_b - \delta_r$ ) of the MD-free region and (ii) the lattice parameter  $a(x_r)$  of the upper part of the buffer; on the other hand, the concentration profile of MDs is determined by the composition profile in the buffers. It is worth noting that if additional structures deposited atop buffers can be considered as single layers with free-standing lattice parameters  $a_a$  (and with a mean composition  $x_a$ ), then, by choosing the

composition profile of buffers, the active structures can be put under overall compressive, null or tensile strain, thus affecting their electronic, optical and transport properties. However, if the lattice parameter of the upper part of the buffer is significantly different from that of the active structure ( $x_r \neq x_a$ ), the latter modifies the strain situation of the buffer that cannot be considered as an independent block any more; in that case, Eq. (1) should be used considering the whole structure consisting of buffer and active region.

We designed structures consisting of graded buffers and two types of MQW structures for 1.3 and 1.5  $\mu\text{m}$  optical modulators, thereafter referred to as 1.3 and 1.5  $\mu\text{m}$  MQWs. The 1.5 and 1.3  $\mu\text{m}$  MQWs both have mean compositions  $x_{\text{MQW}} = 0.34$  and consist of 30.5 periods of 30 and 35  $\text{\AA}$  GaAs barriers and of 65 and 75  $\text{\AA}$  thick  $\text{In}_{0.5}\text{Ga}_{0.5}\text{As}$  wells, respectively. The buffer structures were designed according to Ref. [8, 11] in order to avoid strain in the MQWs; therefore, the composition profiles with linear, square-root and parabolic profiles were graded in 3000 nm up to values  $x_m$  of 0.41, 0.39 and 0.38, respectively, so that  $x_m > x_r = x_{\text{MQW}}$ . It should be noted that this approach is different from that generally used, where the buffer compositions are graded up to the mean compositions of the MQWs ( $x_m = x_{\text{MQW}}$ ), thus resulting in MQWs under compressive strain.

### 4. Results and discussion

Fig. 1 shows a comparison among cross sections of linear, square-root and parabolic buffers; the most interesting features are: (i) it can be clearly seen that the topmost parts of buffers are void of MDs, as predicted by the existing models [6, 8, 10, 11], and as previously observed in Refs. [12, 13], (ii) the thicknesses of MD-free layers increase ranging from linear, square-root and parabolic buffers and are  $\sim 600 \text{ nm}$  for the last ones; the values are in reasonable agreement with the results of Eq. (1) with  $n = 2$ ; (iii) the misfit dislocations have different distributions in buffers with different composition profiles, being almost uniformly distributed (up to  $x_r$ ) in the linear buffers and strongly accumulated towards the

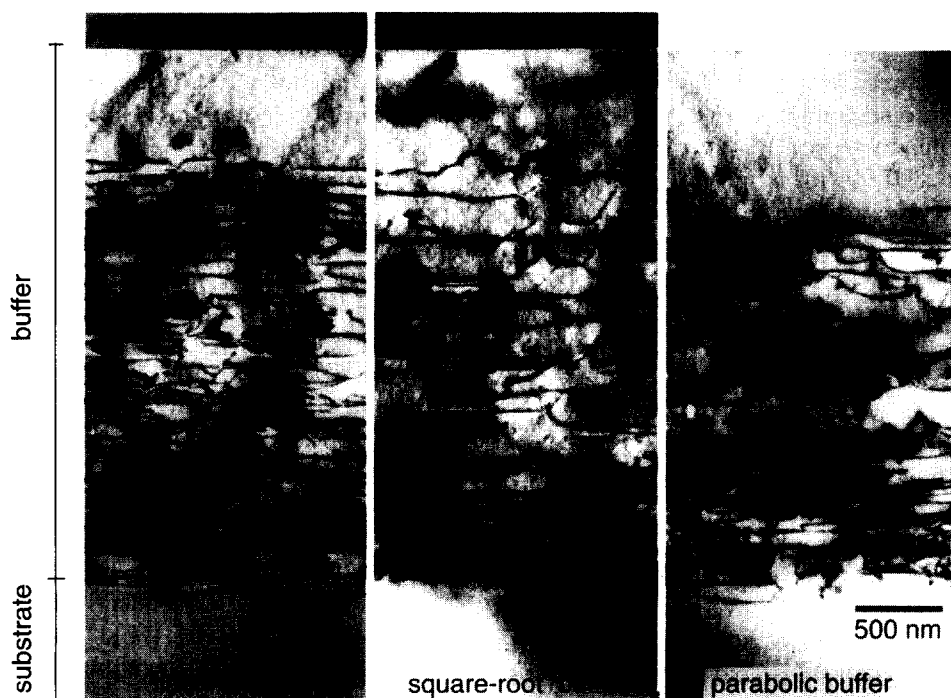


Fig. 1. (110) oriented cross-sectional TEM micrographs of 3000 nm thick InGaAs buffers (grown on (100) GaAs), with linear ( $0.005 \leq x \leq 0.41$ ), square-root ( $0.005 \leq x \leq 0.39$ ) and parabolic ( $0.005 \leq x \leq 0.38$ ) composition profiles.  $g = 220$  type scattering vectors were used.

substrate/buffer interface in square-root buffers; (iv) as predicted by the strain relaxation models [6], continuous grading of composition results in a relatively low concentration of TDs, that in our buffers is lower than  $1 \times 10^6 \text{ cm}^{-2}$ .

When MQWs were grown on the buffers, only a few TDs and MDs at the MQW/buffer interface were found by TEM observations; their maximum density ranged between  $1.5 \times 10^6$  and  $4 \times 10^6 \text{ cm}^{-2}$  for structures with linear and parabolic buffers, respectively. The thicknesses of the MD-free layers in structures with and without MQWs are approximately the same, thus implying that the MQWs do not contribute to the integral of Eq. (1), and, then, that the MQWs are closely lattice-matched to the topmost part of the buffers ( $x_r \sim x_a$ ). Independent of the type of buffer, the MQWs have the same structural quality and interface smoothness (on atomic scale), as those shown in Fig. 2, relative to a MQW grown on a linear buffer.

As an example, in Fig. 3 we show the (004)  $\text{CuK}\alpha$  diffraction profile of a  $1.5 \mu\text{m}$  MQW grown on a square-root buffer; the quality of the structures is assessed by the occurrence of peaks related to MQW periodicity. From the average lattice parameters of MQWs parallel and perpendicular to the interfaces we conclude that the MQWs are nearly lattice matched to the different types of buffers; the In compositions  $x_m$  at the top of buffers evaluated by the diffraction profiles are in good agreement with those derived by using the experimental values of the mean composition of MQWs, the thicknesses of the barriers and wells (obtained by TEM observations) and the In and Ga supply times; it is interesting to note that the  $x_r$  values obtained by Eq. (1) using the above  $x_m$  values are consistent with the strain, whether slightly tensile or compressive, of the MQWs given by HRXRD experiments.

As for the surface smoothness, AFM observations show that both uncapped buffers and MQWs

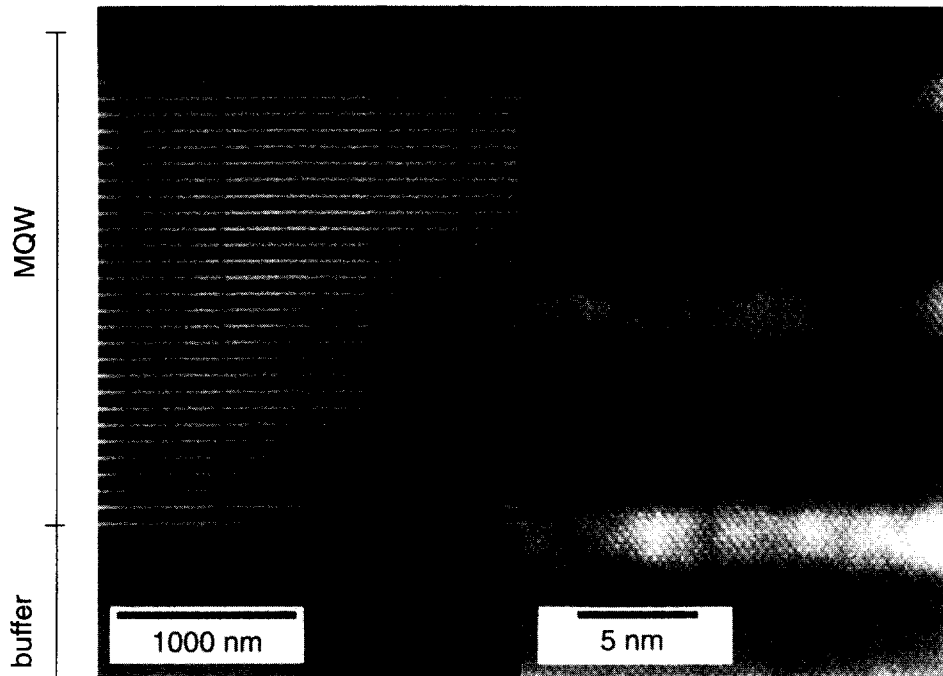


Fig. 2. Dark field,  $g = 002$  type (left panel) and bright field zone axis lattice resolution (right panel) micrographs of a 1.5  $\mu\text{m}$  MQW (30  $\text{\AA}$  GaAs / 65  $\text{\AA}$   $\text{In}_{0.5}\text{Ga}_{0.5}\text{As}$ ) grown atop a linearly graded ( $0.005 \leq x \leq 0.41$ ) InGaAs buffer.

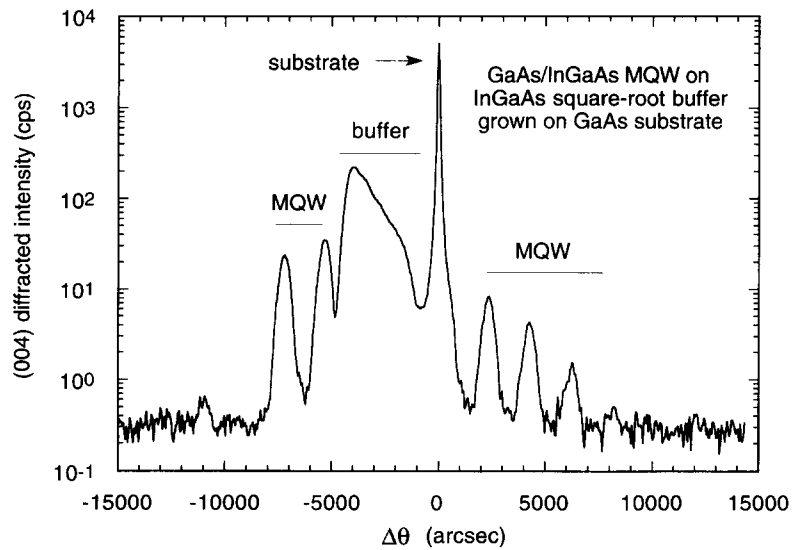


Fig. 3. (0 0 4) CuK $\alpha$  diffraction profile of a 1.5  $\mu\text{m}$  MQW (30  $\text{\AA}$  GaAs / 65  $\text{\AA}$   $\text{In}_{0.5}\text{Ga}_{0.5}\text{As}$ ) grown atop a square-root ( $0.005 \leq x \leq 0.39$ ) InGaAs buffer.

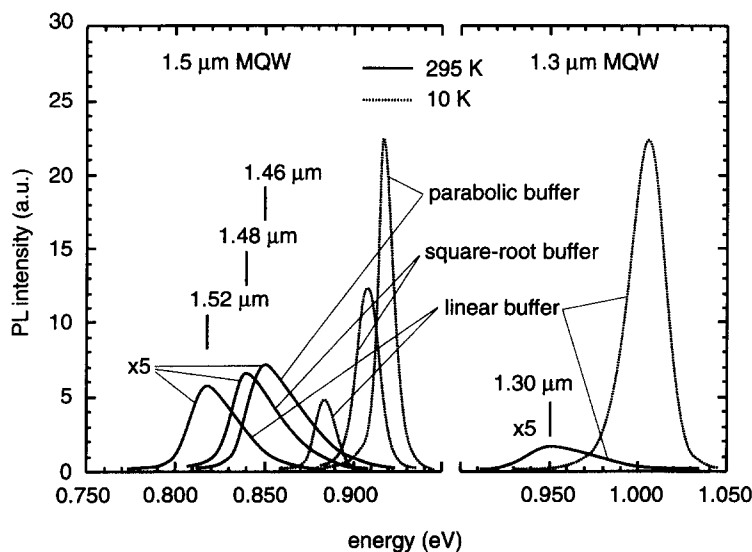


Fig. 4. 10 K and 300 K PL spectra of 1.3 and 1.5  $\mu\text{m}$  MQWs (30  $\text{\AA}$  GaAs / 65  $\text{\AA}$   $\text{In}_{0.5}\text{Ga}_{0.5}\text{As}$  and 35  $\text{\AA}$  GaAs / 75  $\text{\AA}$   $\text{In}_{0.5}\text{Ga}_{0.5}\text{As}$ , respectively), grown on linear ( $0.005 \leq x \leq 0.41$ ), square-root ( $0.005 \leq x \leq 0.39$ ) and parabolic ( $0.005 \leq x \leq 0.38$ ) buffers. The spectral resolution and power densities were 0.5 meV and a  $0.5 \text{ W/cm}^2$ , respectively.

have small and symmetric cross-hatchings along the two orthogonal  $\langle 110 \rangle$ -type directions; the standard deviations of the surface heights (SDSH) depend only slightly on the type of buffer, being, for instance,  $3.4 \pm 0.3$  and  $2.6 \pm 0.3$  nm for linear and parabolic buffers, respectively. The MQWs tend to planarize the surfaces, as can be deduced by the SDSHs of 1.5  $\mu\text{m}$  MQW surfaces that are  $2.0 \pm 0.3$  and  $1.4 \pm 0.2$  nm, for linear and parabolic buffers, respectively.

In Fig. 4 we show the PL spectra at 10 and 300 K of 1.5 and 1.3  $\mu\text{m}$  virtually unstrained MQWs grown on the same buffers as those shown in Fig. 1. It is worth noting that by carefully designing and growing the structures, efficient PL can be obtained at 300 K within or close to the 1.3 and 1.5  $\mu\text{m}$  spectral windows of photonic interest. The PL full-width-at-half-maximums (FWHM) at 10 K relative to the 1.5  $\mu\text{m}$  MQWs (9, 12 and 12 meV, for the parabolic, the square-root and the linear buffers, respectively) are significantly small; this result can be likely related to the design of buffers that virtually do not strain MQWs, unlike the approach that matches the compositions of the tops of buffers to the mean compositions of MQWs. This inter-

pretation may also explain the reduction of the PL FWHMs for increasing  $x_m$  up to values larger than  $x_{\text{MQW}}$  reported in Ref. [14]; our 300 K FWHMs are smaller by a factor of  $\sim 3$ –4 than the 77 K FWHMs given in same paper [14].

## 5. Conclusions

We prepared under optimized conditions and studied InGaAs buffers grown on GaAs, intended for MQW structures for 1.3 and 1.5  $\mu\text{m}$  optical operation at 300 K; the buffers have linear, square-root and parabolic composition profiles. The buffers were designed in such a way that the MQWs grown atop the buffers are virtually unstrained, unlike those prepared following the conventional approach, that are compressively strained. The results obtained by the concomitant use of TEM, HRXRD, AFM and PL show that (i) the MDs profiles and thicknesses of the MD-free regions in the buffers can be predetermined, (ii) the active structures atop buffers are virtually unstrained and have efficient 300 K photoluminescence in the 1.3 and 1.5  $\mu\text{m}$  windows, and (iii) the structures have

TD concentrations in the low  $10^6 \text{ cm}^{-2}$  range and smooth and symmetric cross-hatchings.

### Acknowledgements

The work at MASPEC Institute has been partially supported by the INFN Project RD 23. Thanks are due to P. Allegri, V. Avanzini and M. Scaffardi for technical assistance.

### References

- [1] S.M. Lord, B. Pezeshki, S.D. Kim and J.S. Harris, Jr., *J. Crystal Growth* 127 (1993) 759; S.D. Kim, J.A. Trezza and J.S. Harris, Jr., *J. Vac. Sci. Technol. B* 13 (1995) 1526.
- [2] H.C. Chui, E.L. Martinet, M.M. Fejer and J.S. Harris, Jr., *Appl. Phys. Lett.* 64 (1994) 736; H.C. Chui, S.M. Lord, E. Martinet, M.M. Fejer and J.S. Harris, Jr., *Appl. Phys. Lett.* 63 (1993) 364.
- [3] P. Win, V. Druelle, A. Cappy, Y. Cordier, J. Favre and C. Bouillet, *Appl. Phys. Lett.* 61 (1992) 922.
- [4] T. Uchida, H. Kurakake, H. Soda and S.J. Yamazaki, *J. Electron. Mater.* 25 (1996) 581; H. Ito and J.S. Harris, Jr., *Jpn. J. Appl. Phys.* 12A (1994) 6516.
- [5] E.L. Martinet, H.C. Chui, G.L. Woods, M.M. Fejer, J.S. Harris, Jr., C.A. Rella, B.A. Richman and H.A. Schwettman, *Appl. Phys. Lett.* 65 (1994) 2630.
- [6] J. Tersoff, *Appl. Phys. Lett.* 62 (1993) 693.
- [7] K. Dettmer, U. Behner and R. Beserman, *J. Crystal Growth* 157 (1995) 142.
- [8] G. Salviati, C. Ferrari, L. Lazzarini, S. Franchi, A. Bosacchi, F. Taiariol, M. Mazzer, C. Zanotti-Fregonara, F. Romanato and A.V. Drigo, *Int. Phys. Conf. Series* 146 (1995) 337 (1995).
- [9] M. Madella, A. Bosacchi, S. Franchi, P. Allegri and V. Avanzini, *J. Crystal Growth* 127 (1993) 270.
- [10] A. Sacedón, F. González-Sanz, E. Calleja, E. Muñoz, S.I. Molina, F.J. Pacheco, D. Araújo, R. García, M. Lourenço, Z. Yang, P. Kidd and D. Dunstan, *Appl. Phys. Lett.* 66 (1995) 3334.
- [11] F. Romanato, Study and characterization of compound semiconductor epitaxial layers, PhD Thesis, University of Padova (1994), unpublished.
- [12] A. Bosacchi, A.C. De Riccardis, C. Ferrari, S. Franchi, L. Lazzarini and G. Salviati, MRS Spring Meeting, 8–12 April (1996); S. Francisco, unpublished.
- [13] S.D. Kim, H. Lee and J.S. Harris, Jr., *J. Crystal Growth* 141 (1994) 37.
- [14] H.C. Chui and J.S. Harris, Jr., *J. Vac. Sci. Technol. B* 12 (1994) 1019.